

Sample Targeting During Single-Particle Single-Cell Irradiation

A.W. Bigelow^a, G. Randers-Pehrson^a, K.A. Michel^a, D.J. Brenner^a and A.D. Dymnikov^b

^aCenter for Radiological Research, Columbia University, New York, NY

^bLouisiana Accelerator Center, The University of Louisiana at Lafayette, Lafayette, LA

Abstract. An apertured microbeam is used for single-particle single-cell irradiation to study radiobiological effects at the Radiological Research Accelerator Facility (RARAF), Center for Radiological Research, Columbia University. The present sample targeting system involves imaging techniques and a stepping motor stage to sequentially position a cell nucleus above a vertical ion beam. An interest expressed by the biology research community in targeting subnuclear components has spurred the development of microbeam II, a next-generation facility to include a focused ion beam and a more precise sample manipulator, a voice coil stage. Sample positioning precision will rely on a feedback circuit incorporating linear variable differential transformer (LVDT) position measurements. In addition, post-lens electrostatic deflection is a contender for a point-and-shoot system that could speed up the cell irradiation process for cells within an image frame. Crucial to this development is that ion beam blow up must be minimal during deflection.

INTRODUCTION

The Radiological Research Accelerator Facility (RARAF) at Columbia University is frequently used by biologists to study the effects of radiation on individual mammalian cells. For these experiments an apertured microbeam line was developed to perform controlled single-particle single-cell irradiation. In this highly regulated situation, a biologist can prescribe that a certain percentage of stained cells be irradiated with a certain number of particles, including only one. An overview of the Columbia University single-ion microbeam that also documents the biological interest in the mechanism can be found in a previous article.¹

Presently, the apparatus employs a stepping motor-driven stage. Experimental protocol acquires images through a 4 optical microscope lens of cells plated in a dish mounted to this stage and records their position. During irradiation cell images are acquired again but through a 40 lens and each targeted cell within that frame is sequentially positioned above a 5 μm dia. exit aperture window to a vertical ion beam. This stage positioning has worked well with experiments thus far

as it can target the nucleus of a cell; however, overall positioning error would be a handicap according to upgrade plans for a focused microbeam with submicrometer resolution. Hence, a new sample stage has been developed that meets the next generation resolution requirements. The new stage, dubbed a voice coil stage, utilizes principles similar to those found within sound wave transducers such as microphones or audio speakers. In Addition, frictionless position measurement devices are wired into a closed feedback loop on the voice coil stage to further enhance position accuracy and precision. This new stage will play an important role to satisfy the biology research community's interest in targeting subnuclear cellular components

APPARATUS

Stepping Motor Stage

In order to draw an adequate comparison between the stepping motor stage and the voice coil stage, a

review of the stepping motor stage is useful. The x-y stepping motor-driven stage that is routinely used (Deadal, Inc., Harrison City, PA) was designed to move $0.1 \mu\text{m}$ per step. Although the stage was designed for making submicron steps, positioning limitations are inherent to this type of stage, even after performing an involved optimization of tuning parameters.

Positioning error testing using a similar stepping motor stage from Ludl Corporation measured the location of a fixed object for 50 consecutive $1 \mu\text{m}$ steps. Results of this test are shown in fig. 1, a plot of position errors as a function of distance moved. The plot indicates an overall positioning error of $0.5 \mu\text{m}$ for the Ludl stage compared to $0.2 \mu\text{m}$ for the voice coil stage. In this comparison test, both stages were operating in an open loop mode, without feedback.

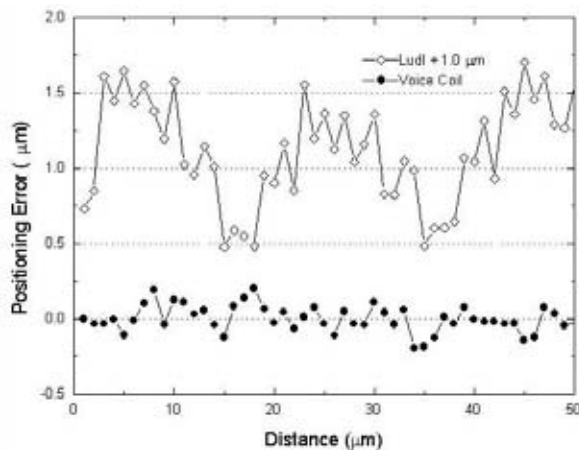


FIGURE 1. Performance comparison of Ludl and voice coil stages.

Voice Coil Stage

The voice coil stage pictured in fig. 2 was developed at Columbia University and weighs about 1 kg. Most of the stage and its frame were made from aluminum. And when possible, excess material was removed from moving components to reduce inertia without compromising rigidity. Flexure mounts (e.g. Kreid 1974) hold together the moving parts; they are robust to the load and the smooth elastic bending motion is favorable to other systems such as bearings. The flexure mount springs are simply thin steel plates; 0.004 in. and/or 0.015 in. thickness. Novel aspects of the voice coil stage are infinitesimal position variability and frictionless position monitors incorporated into a closed feedback loop.

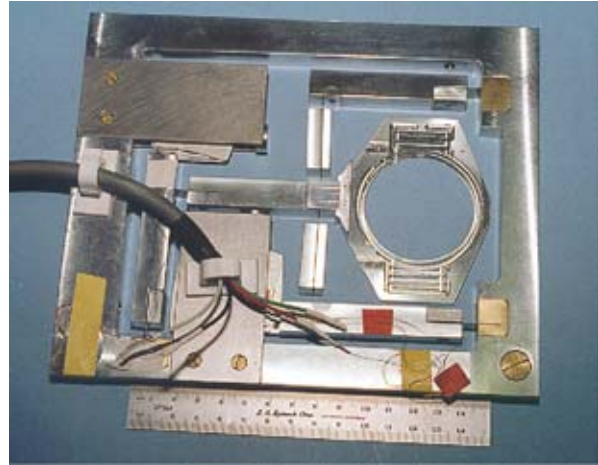


FIGURE 2. Photograph of the voice coil stage.

For this stage, the voice coil concept applies in that each voice-coil drive unit consists of a driving arm with a coil at one end that is set between permanent magnets. When a current flows through the coil, the interaction between the field produced by the coil and that of the permanent magnets causes the arm to move until this force is balanced by the tension in the flex springs connected to the arm. Each coil is approximately rectangular, with inner dimensions of $15 \times 17.5 \text{ mm}$ and outer dimensions of $40 \times 43 \text{ mm}$. They consist of about 400 windings of 34 AWG wire trapped between two aluminum plates attached at the ends of two pivot arms. These current controlled actuators are attractive for their continuous positioning, however, when operated in an open-loop configuration, they are not precise because of hysteresis effects on the flexure mounts.

Closed-loop operation of the voice coil stage is possible with position monitors and feedback circuitry. For this stage, a linear variable differential transformer (LVDT) measures the angular position of a pivot arm. An LVDT has a primary coil centered between two secondary coils, all about a shared axis. A magnetic core positioned within these coils translates an oscillating signal in the primary coil to the secondary coils. The pick-up signal ratio in the secondary coils is a function of the core position. From the dissected view of the LVDT pictured in fig. 3, it was obvious that some physical modifications were necessary to adapt this linear measuring device to a system with angular motion. It was also made clear that there was room to safely enlarge the inner diameter of the coil sensor housing without damaging the windings. So to meet the stage's angular acceptance requirements, half of the coil form material thickness was removed and the core length was shortened to 0.125 in. , despite the vendor's insistence that the cores not be modified.

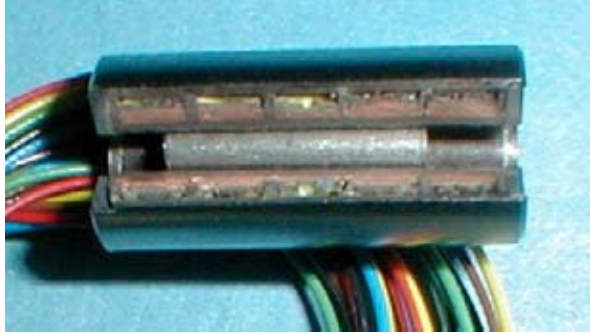


FIGURE 3. Quarter section removed from an LVDT (Schaevitz model 050 MHR) reveals windings, excess inner wall material, and a close fit for the original 0.5 inch long core.

Position response tests for a variety of core lengths were conducted by mounting an LVDT core and sensor to caliper measuring tips. For a series of core positions (0.005 in. increments), voltage signals were read using an AD598, a complete, monolithic LVDT signal conditioning subsystem (Analog Devices). Initial subsystem interconnections followed the data sheet design procedure. For the original core, the LVDT responded linearly across 0.050 in., the advertised measurement range. At the range ends, the electronics saturated at just beyond 10 volts. On the other hand, signal from the shorter core test tended to stray from linearity at range ends. An increase in the gain resistance on the AD598 circuit optimized the linear response range for the short core. To more accurately view the LVDT linear response, a linear fit of the response curve mid section was plotted along with the measurements and the difference between the fit and the measurements. This response curve shown in fig. 4 also portrays an added benefit, an increase in measurement range.

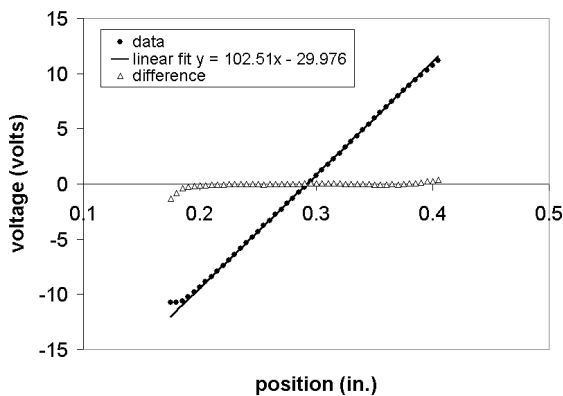


FIGURE 4. Plot of an LVDT short-core response curve using a 150 k gain resistor. The response of this configuration was measured at 3.22 mV/ μ m.

The AD598 data sheet included an electronics schematic for a set-point controller. This circuit was used as a model for the voice coil stage closed loop feedback system; the principle feature is an op amp with negative feedback. Work in progress on this circuit is expected to minimize the stage settling time. Mechanical variables such as spring thickness and eddy current damping (aluminum plates contain the voice coil windings) are important considerations for tuning the feedback system. Under one set of mechanical conditions (0.015 in. thick springs and the use of eddy current damping) the settling time was approximately 100 ns, three times faster than for the present stepping motor stage. Figures 5 and 6 show the frequency response of the AD598 LVDT signal conditioner for the condition mentioned above.

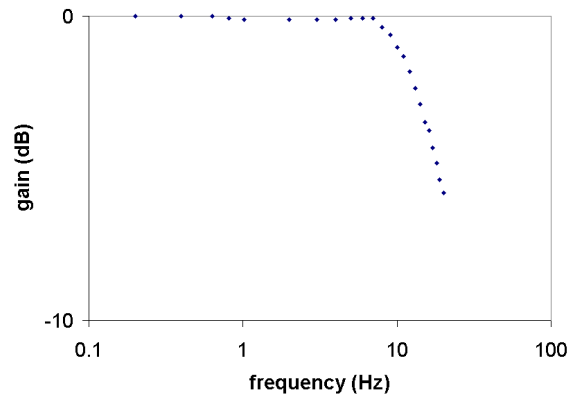


FIGURE 5. Gain characteristics vs. frequency.

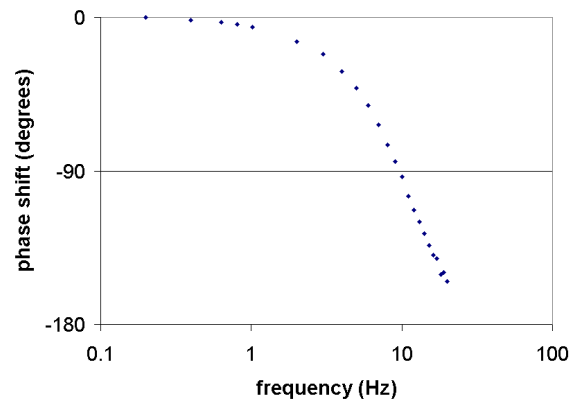


FIGURE 6. Phase characteristics vs. frequency.

A precision evaluation of the voice coil stage stressed the importance for closed loop feedback. One stage control arm was alternately pulled to the side and released. Without feedback, there were significant elastic hysteresis effects. The feedback system improved the positioning error of this alternate-pull test from 2.6 μ m to 0.12 μ m, meeting a goal for

sub-micron resolution. Thin springs (0.004 in.) were set in the stage during this test and the results are shown in fig. 7. Precision error worsened when this test was repeated for the thick spring case. Apparently, the tradeoff is in terms of precision for speed; the thin springs lengthened the stage settling time.

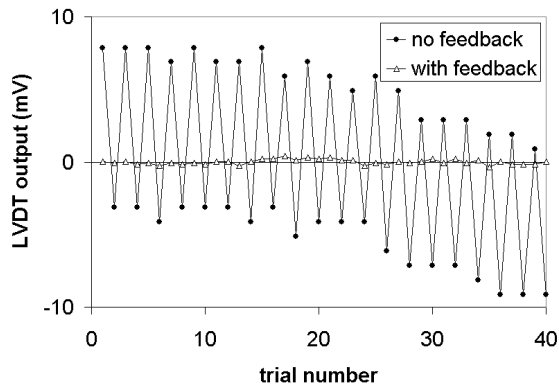


FIGURE 7. Precision trials for the voice coil stage with and without feedback. The voltage to position conversion factor is 3.22 mV/ μm .

Plans for the voice coil stage incorporate its use in on-line and off-line microscopes. Ideal imaging capabilities require that the stage operate consistently under either microscope. The stage frame is designed with a kinetic mount for precision placement each time it is moved between microscopes. The LVDT monitor sets within the walls of the stage frame. And, the plan for the electronics is that they will be imbedded in the frame wall, dedicating one control and feedback circuit for the stage. Again, the overall design goal for this voice coil stage is sub-micron resolution.

POINT-AND-SHOOT ACCESSORY

For both cell-positioning stages discussed above, a time-limiting step is to individually move target cells to just above the vertical ion microbeam. With an upgrade to a focused microbeam, an opportunity arises for a point-and-shoot system, a post-lens accessory that could speed up the irradiation process.

Several electrostatic deflector configurations were simulated with the ion optics package, SIMION.² The amount of beam enlargement was too great for rod electrode geometry, but was acceptable/negligible for parallel plates.³ The simulation of the plate deflectors is shown in fig. 8 and an encouraging comparison of ion beam profile histograms is shown in fig. 9.

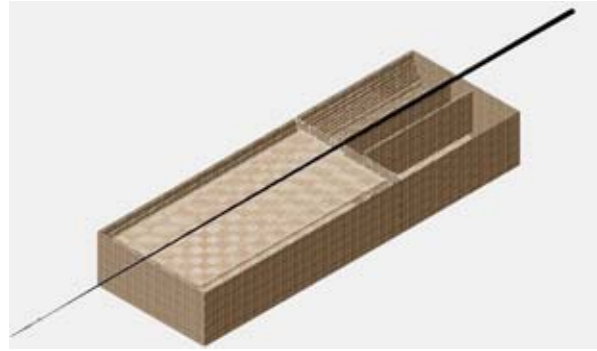


FIGURE 8. Half view of the deflector plate simulation. Plate lengths are in sequence 20 mm and 35 mm, the plate gap is 4 mm and the tube diameter is 20 mm. For 6 MeV alpha particles, the pointing requirement is 1000 V/100 μm at the target 21 mm after the exit of the deflector.

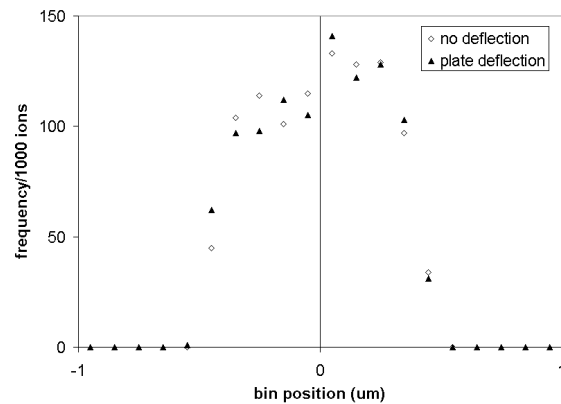


FIGURE 9. Simulated ion beam profiles taken at the target plane. For comparison, the deflected beam coordinates are superimposed onto the non-deflected beam. This point-and-shoot system would apply to cells within one 40 lens view.

ACKNOWLEDGMENTS

This work was supported in part by NIH grants RR-11623 and CA-49062.

REFERENCES

1. Randers-Pehrson, G., Geard, C.R., Johnson, G., Elliston, C.D., and Brenner, D.J. *Radiation Research* **156**, (2001) 210-214.
2. Idaho National Engineering and Environmental Laboratory, Idaho Falls, ID 83415.
3. Moretto, Ph., Michelet, C., Balana, A., Barberet, Ph., Przybylowicz, W.J., Slabbert, J.P., Prozesky, V.M., Pineda, C.A., Brut, G., Laurent, G., Lhoste, F., *Nucl. Instr. and Meth.B* **181** (2001) 104-109.